[^{13}C]-constant-time [^{15}N,^{1}H]-TROSY-HNCA for sequential assignments of large proteins

Michael Salzmann[a,b], Konstantin Pervushin[a], Gerhard Wider[a], Hans Senn[b] & Kurt Wüthrich[a,*]

[a]*Institut für Molekularbiologie und Biophysik, Eidgenössische Technische Hochschule Hönggerberg, CH-8093 Zürich, Switzerland*
[b]*F. Hoffmann-La Roche AG, Pharma Research, CH-4070 Basel, Switzerland*

Abstract

The greatly improved sensitivity resulting from the use of TROSY during ^{15}N evolution and amide proton acquisition enables the recording of HNCA spectra of large proteins with constant-time ^{13}C$^{\alpha}$ evolution. In [^{13}C]-ct-[^{15}N,^{1}H]-TROSY-HNCA experiments with a ^{2}H/^{13}C/^{15}N-labeled 110 kDa protein, 7,8-dihydroneopterin aldolase from *Staphylococcus aureus*, nearly all correlation peaks seen in the [^{15}N,^{1}H]-TROSY-HNCA spectrum were also detected. The improved resolution in the ^{13}C dimension then enabled a significant number of sequential assignments that could not be obtained with [^{15}N,^{1}H]-TROSY-HNCA without [^{13}C]-constant-time period.

Abbreviations: CSA, chemical shift anisotropy; ct, constant-time; DD, dipole–dipole; INEPT, insensitive nuclei enhanced by polarization transfer; PFG, pulsed field gradient; rf, radio-frequency; ST2-PT, single transition-to-single transition polarization transfer; 3D, three-dimensional; TPPI, time-proportional phase incrementation; TROSY, transverse relaxation-optimized spectroscopy.

Introduction

Assignment of chemical shifts to individual nuclei provides the foundation for protein structure determination by NMR (Wüthrich et al., 1982; Wüthrich, 1986), and hence obtaining sequence-specific resonance assignments for larger proteins is a necessary requirement for further extension of the size limit for NMR structure determination. Multidimensional triple-resonance NMR experiments with ^{2}H/^{13}C/^{15}N-labeled proteins have so far been the most successful approach in this regard (LeMaster, 1994; Yamazaki et al., 1994a,b; Shan et al., 1996; Kay and Gardner, 1997; Gardner et al., 1998), and with the introduction of TROSY (Pervushin et al., 1997) into triple resonance experiments (Salzmann et al., 1998, 1999) the potentialities of this approach have been further largely extended. With the constructive use of the in-

terference between dipole–dipole (DD) coupling and chemical shift anisotropy (CSA) interactions in ^{15}N–^{1}H^{N} moieties, up to three-fold sensitivity gains were obtained using TROSY-type triple resonance experiments with a 23 kDa protein when compared to the corresponding conventional implementations (Salzmann et al., 1998, 1999; Yang and Kay, 1999). In large proteins, full use of the improved sensitivity is limited by signal overlap in the ^{13}C dimension, which may prevent unique correlation of backbone ^{15}N–^{1}H^{N} groups with the intraresidually and sequentially adjoining ^{13}C$^{\alpha}$, ^{13}C$^{\beta}$ or ^{13}CO spins. Since the spin-selective state of ^{15}N can be preserved during a [^{13}C]-constant-time (ct) evolution period, the improved sensitivity due to the use of TROSY now opens an avenue to overcome this limitation by introducing ct ^{13}C evolution periods, which eliminate homonuclear ^{13}C–^{13}C scalar couplings and provide much narrower lines in the ^{13}C dimension (Vuister and Bax, 1992; Yamazaki,

---

*To whom correspondence should be addressed.
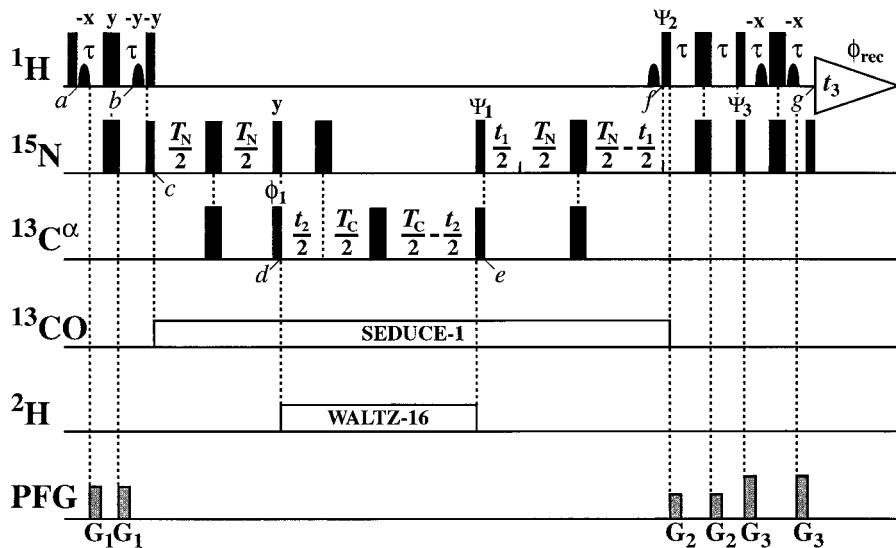
Figure 1. Experimental scheme for the $[^{13}C]$-ct-$[^{15}N,^1H]$-TROSY-HNCA experiment for deuterated proteins (for the modifications needed for protonated proteins, see Salzmann et al., 1998). The radio-frequency (rf) pulses on ^1H, ^{15}N, ^{13}CO, $^{13}C^\alpha$ and ^2H were applied at 4.8, 119, 174, 55 and 3.8 ppm, respectively. The narrow and wide black bars indicate non-selective 90° and 180° pulses, respectively. On the line marked ^1H, sine bell shapes indicate selective 90° pulses with a duration of 1 ms and a Gaussian shape truncated at 5%, which are applied on the water resonance. The line marked PFG indicates durations and amplitudes of Gaussian shape pulsed magnetic field gradients applied along the z-axis: G_1: 800 μs, 15 G/cm; G_2: 800 μs, 9 G/cm; G_3: 800 μs, 22 G/cm. The delays are $\tau = 2.7$ ms, $T_N = 18.2$ ms and $T_C = 26.2$ ms. The phase cycle is $\Psi_1 = \{y, -y, x, -x\}$, $\Psi_2 = \{-y\}$, $\Psi_3 = \{-y\}$, $\phi_1 = \{4x, 4(-x)\}$ and $\phi_{rec} = \{y, -y, -x, x, -y, y, x, -x\}$. All other rf-pulses are applied either with phase x or as indicated above the pulses. In the $^{15}N(t_1)$ dimension a phase-sensitive spectrum is obtained by recording a second FID for each increment of t_1, with $\Psi_1 = \{y, -y, -x, x\}$; $\Psi_2 = \{y\}$; $\Psi_3 = \{y\}$, and the data is processed as described by Kay et al. (1992). Quadrature detection in the $^{13}C^\alpha(t_2)$ dimension is achieved by the States-TPPI method (Marion et al., 1989) applied to the phase ϕ_1. The water magnetization stays aligned along the $+z$-axis throughout the experiment by the use of water flip-back pulses (Grzesiek and Bax, 1993) at times a, b and f. Residual transverse water magnetization is suppressed by the WATERGATE sequence (Piotto et al., 1992) immediately before data acquisition. For ^2H-decoupling, WALTZ-16 (Shaka et al., 1983) was used with a field strength of 2.5 kHz. ^{13}CO decoupling was performed using off-resonance SEDUCE-1 (McCoy and Mueller, 1992) with a field strength of 0.83 kHz, which allows the application of rf-pulses on the $^{13}C^\alpha$ channel with a field strength of 20.83 kHz.

1994a). This communication describes an implementation of $[^{13}C]$-ct-$[^{15}N,^1H]$-TROSY-HNCA and its application with a $^2H/^{13}C/^{15}N$-labeled 110 kDa protein, the 7,8-dihydroneopterin aldolase from *Staphylococcus aureus* (Hennig et al., 1998).

A 3D HNCA experiment yields two $^{13}C^\alpha$ correlation peaks for each $^{15}N(i)-^1H^N(i)$ amide moiety, the intraresidual peak with $^{13}C^\alpha(i)$ and the sequential peak with $^{13}C^\alpha(i-1)$, so that for larger proteins one ends up with a crowding of cross peaks along the ^{13}C frequency axis (Montelione and Wagner, 1989; Ikura et al., 1990; Grzesiek and Bax, 1992). In the implementation of the HNCA or $[^{15}N,^1H]$-TROSY-HNCA experiments one works with limited resolution in the ^{13}C dimension to prevent that the homonuclear scalar couplings between $^{13}C^\alpha$ and $^{13}C^\beta$ are resolved (Wider, 1998). The introduction of a $[^{13}C]$-ct evolution period of duration $T_C = 1/^1J(^{13}C^\alpha,^{13}C^\beta)$ enables a three-fold increase in resolution for the $^{13}C^\alpha$ dimension without the appearance of $^{13}C^\alpha-^{13}C^\beta$ couplings,

and the carbonyl carbons can in any case readily be decoupled from $^{13}C^\alpha$ by selective composite pulse decoupling (McCoy and Mueller, 1992). The use of a $[^{13}C]$-ct evolution period, however, increases the time period during which transverse $^{13}C^\alpha$ magnetization is active by approximately 20 ms. In view of the concomitant loss of sensitivity, we present here an initial application with the intrinsically highly sensitive $[^{15}N,^1H]$-TROSY-HNCA experiment (Salzmann et al., 1998), using uniformly deuterated proteins.

Figure 1 shows an experimental scheme for $[^{13}C]$-ct-$[^{15}N,^1H]$-TROSY-HNCA, where TROSY is implemented as recently described (Salzmann et al., 1998, 1999). Both the ^1H and ^{15}N steady-state magnetizations are used at the outset of the experiment (Pervushin et al., 1998a,b). Between the time points a and d, the magnetization is transferred from $^1H^N$ via ^{15}N to $^{13}C^\alpha$, using two successive INEPT steps. During the $[^{13}C]$-ct evolution period, $^{13}C^\alpha$ evolves due to the $^{13}C^\alpha$ chemical shift only, since ^{13}CO, ^{15}N and
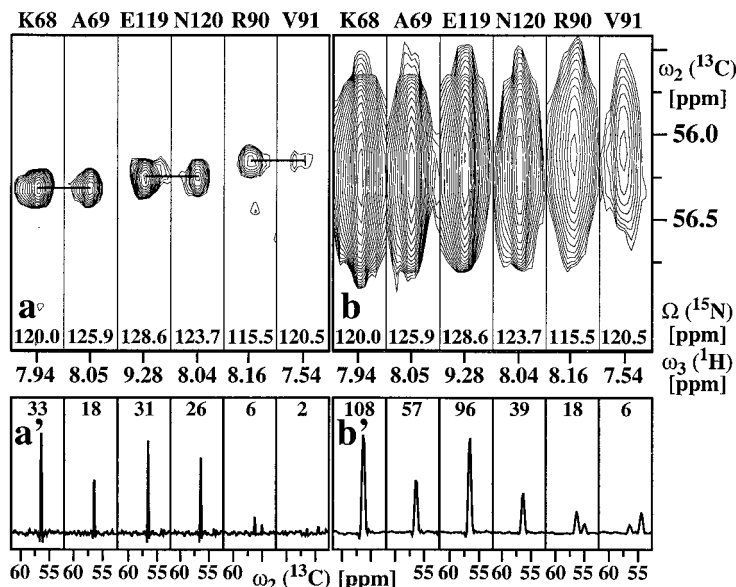
Figure 2. Comparison of corresponding $[\omega_2(^{13}C),\omega_3(^{1}H)]$ strips from HNCA spectra obtained with and without ^{13}C constant time evolution: (a) $[^{13}C]$-ct-$[^{15}N,^{1}H]$-TROSY-HNCA recorded with the scheme of Figure 1; (b) $[^{15}N,^{1}H]$-TROSY-HNCA (Salzmann et al., 1998). The strips were taken at the ^{15}N chemical shifts indicated at the bottom, and are centered about the corresponding $^{1}H^{N}$ chemical shifts. At the top the sequence-specific assignments are indicated by the one-letter amino acid symbol and the sequence number. In (a) the three sequential connectivities are indicated by horizontal lines. (a′) and (b′) show cross sections along the $\omega_2(^{13}C)$ dimension through the centers of the strips in (a) and (b), respectively, where the chemical shift range from 52 to 62 ppm is plotted. The signal-to-noise ratios for the main peak in each cross section are indicated at the top. Both spectra were recorded at 20 °C with the same 0.5 mM sample of uniformly $^{2}H/^{13}C/^{15}N$-labeled 7,8-dihydroneopterin aldolase from *S. aureus* (Hennig et al., 1998) in a mixed solvent of 95% H_2O/5% D_2O at pH 6.5, using a Bruker DRX-750 spectrometer equipped with four rf channels for generating the ^{1}H, ^{2}H, ^{13}C and ^{15}N rf-pulses, a pulsed field gradient unit and a triple resonance probehead with an actively shielded z-gradient coil. When recording the spectrum (b), the previous implementation of the $[^{15}N,^{1}H]$-TROSY-HNCA experiment (Salzmann et al., 1998) was modified so that ^{13}CO decoupling by Gaussian off-resonance pulses was replaced by 0.83 kHz off-resonance SEDUCE-1 decoupling (McCoy and Mueller, 1992) and the rf-pulses on the $^{13}C^{\alpha}$ channel were applied with a field strength of 20.83 kHz, exactly as described for $[^{13}C]$-ct-$[^{15}N,^{1}H]$-TROSY-HNCA in Figure 1. The following parameter settings were used for (a): data size $42(t_1) \times 128(t_2) \times 1024(t_3)$ complex points; $t_{1max}(^{15}N) = 17.4$, $t_{2max}(^{13}C^{\alpha}) = 25.6$, $t_{3max}(^{1}H) = 75.6$ ms; spectral widths in $\omega_1(^{15}N)$, $\omega_2(^{13}C^{\alpha})$ and $\omega_3(^{1}H)$ 2400, 5000 and 13550 Hz, respectively; 16 scans per increment were acquired, resulting in 4 days of measuring time. The data set was zero-filled to $128(t_1) \times 256(t_2) \times 2048(t_3)$ complex points. In (b) the same parameters were used except for the following: data size in t_2 was 40 points, $t_{2max}(^{13}C^{\alpha}) = 8$ ms, 48 scans per increment were acquired in 4 days of measuring time, and zero-filling in t_2 was to 128 complex points. Prior to Fourier transformation both data matrices were multiplied with a 75°-shifted sine bell window in the indirect dimensions and a 60°-shifted sine bell window in the acquisition dimension (DeMarco and Wüthrich, 1976). Data processing was performed using the program PROSA (Güntert et al., 1992), and for the data analysis the program XEASY (Bartels et al., 1995) was used.

^{2}H are decoupled during t_2, and T_C is chosen such that $T_C = 1/^{1}J(^{13}C^{\alpha},^{13}C^{\beta})$ (Vuister and Bax, 1992). The magnetization is transferred back to ^{15}N at time point *e*. Between *e* and *f* the ^{15}N nuclei evolve with their chemical shifts during a ct period, and from time point *f* onward the ST2-PT element transfers the ^{15}N single-transition to the ^{1}H single transition selected in TROSY (Pervushin et al., 1998a). The water magnetization is maintained along the $+z$-axis during the entire experiment, using selective pulses on the water resonance at the time points *a*, *b* and *f* (Grzesiek and Bax, 1993). The coherence flow in $[^{13}C]$-ct-$[^{15}N,^{1}H]$-TROSY-HNCA can thus be described by

$$H_i \rightarrow \underline{N_i} \rightarrow C_{i,i-1}^{\alpha}(t_2) \rightarrow \underline{N_i(t_1)} \rightarrow \underline{H_i(t_3)} \quad (1)$$

where H, N and C^{α} represent the $^{1}H^{N}$, ^{15}N and $^{13}C^{\alpha}$ magnetizations, t_1 and t_2 are the ^{15}N and ^{13}C evolution times, and t_3 is the ^{1}H acquisition time. The indices i and $i-1$ indicate that coherence is transferred from $^{15}N(i)$–$^{1}H^{N}(i)$ to both the sequentially and the intraresidually adjoining $^{13}C^{\alpha}s$. The periods during which TROSY is active are underlined: on ^{15}N it is active during the ^{15}N–$^{13}C^{\alpha}$ INEPT and the reverse $^{13}C^{\alpha}$–^{15}N INEPT, including the ct ^{15}N evolution period t_1, and on $^{1}H^{N}$ it acts during the data acquisition period t_3. During the $[^{13}C]$-ct evolution period the ^{15}N spin-selective state is preserved. In principle,

the pulse sequence of Figure 1 could be adapted for use with protonated proteins by replacing deuterium decoupling with selective decoupling of the α-protons (Salzmann et al., 1998), but fast $^{13}C^\alpha$ relaxation will limit such applications.

Figure 2, a and b, shows corresponding $[\omega_2(^{13}C),\omega_3(^1H)]$ strips from 3D $[^{13}C]$-ct-$[^{15}N,^1H]$-TROSY-HNCA and 3D $[^{15}N,^1H]$-TROSY-HNCA spectra of a uniformly $^2H/^{13}C/^{15}N$-labeled protein recorded with identical conditions. The protein studied is the 7,8-dihydroneopterin aldolase from *Staphylococcus aureus*, which has a molecular weight of 110 kDa and consists of eight identical subunits with 121 amino acid residues. The protein concentration was 0.5 mM, i.e., 4 mM in subunits. From measurements of $T_1(^{15}N)/T_2(^{15}N)$ we obtained an estimate for the lower limit on the effective rotational correlation time at 20 °C of $\tau_c \geq 45$ ns (Kay et al., 1989). The strips were taken at the ^{15}N chemical shifts of the residues 68, 69, 119, 120, 90 and 91, and the horizontal lines in Figure 2a indicate the sequential connectivities for the three pairs of neighboring residues. The improved spectral resolution in $[^{13}C]$-ct-$[^{15}N,^1H]$-TROSY-HNCA enabled the unambiguous identification of the sequential $^1H^N$–$^{13}C^\alpha$ connectivities in the crowded $^{13}C^\alpha$ frequency range around 56 ppm, whereas with $[^{15}N,^1H]$-TROSY-HNCA no reliable sequential assignment was possible because of spectral overlap (Figure 2b).

The $[^{13}C]$-ct period in $[^{15}N,^1H]$-TROSY-HNCA is of special interest for large proteins with crowded spectra (Gardner et al., 1998). In spite of the decrease of signal-to-noise (see Figure 2, a′ and b′), a workable sensitivity is maintained. For example, in the presently studied aldolase one expects 117 intraresidual and 117 sequential HNCA cross peaks. The numbers of peaks seen by $[^{15}N,^1H]$-TROSY-HNCA were 117 and 114, and by $[^{13}C]$-ct-$[^{15}N,^1H]$-TROSY-HNCA they were 110 and 103, i.e., 94% of all expected intraresidual and 88% of all expected sequential peaks were seen using 3D $[^{13}C]$-ct-$[^{15}N,^1H]$-TROSY-HNCA.

Acknowledgements

References

Bartels, C., Xia, T., Billeter, M., Güntert, P. and Wüthrich, K. (1995) *J. Biomol. NMR*, **6**, 1–10.

DeMarco, A. and Wüthrich, K. (1976) *J. Magn. Reson.*, **24**, 201–204.

Gardner, K.H., Zhang, X., Gehring, K. and Kay, L.E. (1998) *J. Am. Chem. Soc.*, **120**, 11738–11748.

Grzesiek, S. and Bax, A. (1992) *J. Magn. Reson.*, **96**, 432–440.

Grzesiek, S. and Bax, A. (1993) *J. Am. Chem. Soc.*, **115**, 12593–12594.

Güntert, P., Dötsch, V., Wider, G. and Wüthrich, K. (1992) *J. Biomol. NMR*, **2**, 619–629.

Hennig, M., D'Arcy, A., Hampele, I.C., Page, M.G.P., Oefner, C. and Dale, G.E. (1998) *Nat. Struct. Biol.*, **5**, 357–362.

Ikura, M., Kay, L.E. and Bax, A. (1990) *Biochemistry*, **29**, 4659–4667.

Kay, L.E., Torchia, D.A. and Bax, A. (1989) *Biochemistry*, **28**, 8972–8979.

Kay, L.E., Keifer, P. and Saarinen, T. (1992) *J. Am. Chem. Soc.*, **114**, 10663–10664.

Kay, L.E. and Gardner, K.H. (1997) *Curr. Opin. Struct. Biol.*, **7**, 722–731.

LeMaster, D.M. (1994) *Prog. NMR Spectrosc.*, **26**, 371–419.

Marion, D., Ikura, M., Tschudin, R. and Bax, A. (1989) *J. Magn. Reson.*, **85**, 393–399.

McCoy, M.A. and Mueller, L. (1992) *J. Am. Chem. Soc.*, **114**, 2108–2112.

Montelione, G.T. and Wagner, G. (1989) *J. Am. Chem. Soc.*, **111**, 5474–5475.

Pervushin, K., Riek, R., Wider, G. and Wüthrich, K. (1997) *Proc. Natl. Acad. Sci. USA*, **94**, 12366–12371.

Pervushin, K., Riek, R., Wider, G. and Wüthrich, K. (1998a) *J. Am. Chem. Soc.*, **120**, 6394–6400.

Pervushin, K., Wider, G. and Wüthrich, K. (1998b) *J. Biomol. NMR*, **12**, 345–348.

Piotto, M., Saudek, V. and Sklenar, V.J. (1992) *J. Biomol. NMR*, **2**, 661–665.

Salzmann, M., Pervushin, K., Wider, G., Senn, H. and Wüthrich, K. (1998) *Proc. Natl. Acad. Sci. USA*, **95**, 13585–13590.

Salzmann, M., Wider, G., Pervushin, K., Senn, H. and Wüthrich, K. (1999) *J. Am. Chem. Soc.*, **121**, 844–848.

Shaka, A.J., Keeler, J., Frenkiel, T. and Freeman, R. (1983) *J. Magn. Reson.*, **52**, 335–338.

Shan, X., Gardner, K.H., Muhandiram, D.R., Rao, N.S., Arrowsmith, C.H. and Kay, L.E. (1996) *J. Am. Chem. Soc.*, **118**, 6570–6579.

Vuister, G.W. and Bax, A. (1992) *J. Magn. Reson.*, **98**, 428–435.

Wider, G. (1998) *Prog. NMR Spectrosc.*, **32**, 193–275.

Wüthrich, K., Wider, G., Wagner, G. and Braun, W. (1982) *J. Mol. Biol.*, **155**, 311–319.

Wüthrich, K. (1986) *NMR of Proteins and Nucleic Acids*, Wiley, New York, NY.

Yamazaki, T., Lee, W., Revington, M., Mattiello, D.L., Dahlquist, F.W., Arrowsmith, C.H. and Kay, L.E. (1994a) *J. Am. Chem. Soc.*, **116**, 6464–6465.

Yamazaki, T., Lee, W., Arrowsmith, C.H., Muhandiram, D.R. and Kay, L.E. (1994b) *J. Am. Chem. Soc.*, **116**, 11655–11666.

Yang, D. and Kay, L.E. (1999) *J. Biomol. NMR*, **13**, 3–10.